Journal of Molecular Structure 1245 (2021) 130993

Contents lists available at ScienceDirect

Journal of Molecular Structure

journal homepage: www.elsevier.com/locate/molstr

Preparation, structure determination, and in silico and in vitro Elastase inhibitory properties of substituted *N*-([1,1′-Biphenyl]-2-ylcarbamothioyl)- Aryl/Alkyl benzamide Derivatives

Sara Ilyas[a], Aamer Saeed[a,*], Qamar Abbas[b], Rabail Ujan[a], Pervaiz Ali Channar[a], Izhar Ahmed Shaikh[c], Mubashir Hassan[d], Hussain Raza[e], Sung-Yum Seo[e], Gustavo A. Echeverría[f], Oscar E. Piro[f], Mauricio F. Erben[g,*]

[a] Department of Chemistry, Quaid-I-Azam University, Islamabad 45320, Pakistan
[b] Department of Biology, College of Science, University of Bahrain, Sakhir, 32038 Kingdom of Bahrain
[c] Department of PCSIR head office ministry of science and technology Islamabad, Pakistan
[d] Institute of Molecular Biology and Biotechnology/(IMBB), The University of Lahore, 1-KM, Defense Road, Bhubtian Chowk, Lahore, Pakistan
[e] Department of Biological Sciences, College of Natural Sciences, Kongju National University, 56 Gongjudehak-Ro, Gongju, Chungnam 314-701, Republic of Korea
[f] Departamento de Física, Facultad de Ciencias Exactas, Universidad Nacional de La Plata e Instituto de Física La Plata, IFLP (UNLP, CONICET, CCT-La Plata), C. C. 67, 1900 La Plata, Argentina
[g] CEQUINOR (UNLP-CONICET, CCT-La Plata), Departamento de Química, Facultad de Ciencias Exactas, Universidad Nacional de La Plata, Boulevard 120 e/ 60 y 64 Nº 1465 La Plata B1900, Buenos Aires, Argentina

ARTICLE INFO

Article history:
Received 19 May 2021
Revised 14 June 2021
Accepted 26 June 2021
Available online 14 July 2021

Keywords:
Aryl thioureas
Structural X-ray diffraction
Biological activity
Docking studies
Elastase inhibition activity

ABSTRACT

The preparation of a set of eight closely related biphenyl-thiourea conjugates with aromatic and aliphatic side chains (**3a-3h**) using a one-pot three-component strategy is reported. All the novel compounds were characterized by spectroscopic techniques (FTIR, ^{1}H and ^{13}C NMR) and elemental analysis. Moreover, the crystal structure of compounds **3f** and **3h** have been determined by X-ray diffraction. The common molecular skeleton can be closely superposed to each other and the 1-acyl thiourea groups show a nearly planar conformation favored by an intramolecular N–H•••O=C bond. In-vitro studies were carried out to test the elastase inhibition activity of the newly synthesized biphenyl-thiourea hybrid derivatives. Among the series, compound **3c** ($IC_{50} = 0.26 \pm 0.05\ \mu M$) exhibited the maximum inhibition against elastase. The higher activity of aryl substituents over alkyl chains is evidenced, as well as the importance of electron withdrawing groups, as nitro (**3b** and **3c**) and bromo (**3d**) to enhance the enzyme inhibitory activity. The compound **3c** inhibits the enzyme in a competitive manner, with dissociation constant $K_i = 0.84$ µM. Molecular docking was also carried out within the enzyme active site to study enzyme-inhibitor interactions. Docking results correlate with experimental inhibition studies and show that compound **3c** exhibits the highest binding energy (-7.70 kcal/mol) as compared with other compounds. The results of this study might help to develop new elastase inhibitors.

1. Introduction

Acyl thiourea compounds are currently receiving considerable attention because of their wide applications in several fields [1]. The straightforward synthetic route and excellent properties are the important features which engage many researchers in efforts to explore more such multipurpose thio compounds [2,3]. A wide range of 1-(acyl/aroyl)-3-(substituted) thioureas are extremely versatile starting materials for the synthesis of a variety of heterocyclic compounds due to the presence of two hydrogen atoms bonded to each of the nitrogen atoms [4]. Moreover, an array of pharmacological properties associated with 1-(acyl/aroyl)-3-(substituted)thioureas has made them attractive templates for future drug design. Thiourea and urea derivatives show a broad spectrum of biological activities such as antitumor [5], herbicidal [6], antiviral [7], antiparasitic [8], antimi-

* Corresponding authors.
E-mail addresses: aamersaeed@yahoo.com (A. Saeed), erben@quimica.unlp.edu.ar (M.F. Erben).

https://doi.org/10.1016/j.molstruc.2021.130993
0022-2860/

crobial [9], insecticidal [10], pesticidal and fungicidal properties [11,12]. Thus, 1-acyl-3-(2-amino-phenyl) thioureas exhibit anti-intestinal nematode activity [13], the thiourea derivatives of 4-azatricyclo[5.2.2.02,6]undec-8-ene-3,5-dione [14] and pyridazine [15]; 1-aroyl-3-(substituted-2-benzothiazolyl)thioureas [16] and 1-aroyl-3-arylthioureas [17] exhibit potent antibacterial activity. *N*-Phenyl and *N*-benzoyl thioureas are antimicrobial agents [18] and excellent antifungal activity were reported for fluorinated thioureas [19].

In addition, biphenyl derivatives are used in the synthesis of antifungal agents like bifonazole, optical brightening agents, dyes, and polychlorinated biphenyls (PCBs). In particular, biphenyl thioureas have been used as organocatalysts for electrochemical reductions [20].

Few structures containing the biphenyl-thiourea scaffold can be found in the literature, the list includes the *N*-(biphenyl-4-carbonyl)-*N* -(4-chlorophenyl)thiourea [21], its 2-chloro- [22], 2-pyridylmethyl)- [23], and 6-methylpyridin-2-yl [24] analogues. In these cases, the thiourea scaffold is formed from the corresponding biphenyl isothiocyanate. Then, as a first objective of this work, we wanted to know the capability of using the carbonyl isothiocyanate route for preparing acyl/aryl-carbonyl biphenyl thioureas. A second aim is to determine how different substituent affects the structural properties around the central 1-acyl thiourea group [25]. Finally, the investigation of biological properties is also undertaken in continuation of our studies on sulfur organic compounds [26,27]. Thus, considering the aforesaid significance of thiourea motif and the multifunctional value of biphenyl group, the aim of the current work was the synthesis of thiourea species containing the biphenyl group in a single structural entity. Eight close related compounds were prepared and characterized by FTIR and multinuclear (^{1}H and ^{13}C) NMR spectroscopy. The X-ray single crystal structure of two compounds were determined. Furthermore, the synthesized compounds were screened against elastase enzyme to examine biological activity, rationalized by kinetic measurements and computational docking studies.

2. Experimental

Melting points were recorded using a digital Gallenkamp (SANYO) model MPD.BM 3.5 apparatus and are uncorrected. ^{1}H and ^{13}C NMR spectra were determined in $CDCl_3$ at 300 MHz and 75.4 MHz, respectively, using a Bruker spectrophotometer. FTIR spectra were recorded on an FTS 3000 MX spectrophotometer. Elemental analyses were conducted using a LECO-183 CHNS analyzer.

2.1. General Procedure for the synthesis *N*-([1,1′-Biphenyl]-2-ylcarbamothioyl)-4-alkyl/arylbenzamides (**3a-3h**)

In freshly prepared solution of potassium thiocyanate (1.65 mmol) in dry acetone (15 ml) solution of substituted acid chloride (1.1 mmol) **(1)** was added dropwise in a round bottom flask. Then refluxed the reaction mixture for 2h under nitrogen atmosphere. Milky appearance indicated the acyl thiocyanate formation. The reaction mixture could cool at room temperature and a solution of 2-aminobiphenyl (1.1 mmol) in acetone was added dropwise in the reaction mixture and refluxed it again for 3h. On the reaction completion, monitored by TLC, the reaction mixture was cooled to room temperature and then poured into crushed ice. The precipitated thioureas were filtered dried and recrystallized from acetone.

N-([1,1′-Biphenyl]-2-ylcarbamothioyl)-4-methylbenzamide (3a)

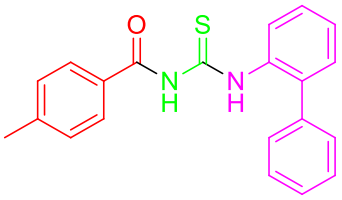

White solid, m.p.: 181-183 °C, Yield= 82 %, R_f= 0.51 (n-Hexane: Ethyl acetate 4:1); IR (KBr, v/cm^{-1}): 3350 (NH), 3143 (NH), 1650 (C=O), 1579, 1473 (C=C aromatic), 1253 (C=S); ^{1}H NMR ($CDCl_3$, 300 MHz,); δ (ppm): 11.81 (s, 1H, NH), 9.41 (s, 1H, NH), 7.91 (d, 2H, J=7.9 Hz, Ar–H), 7.43 (d, 2H, J=7.8 Hz, Ar–H), 7.32-7.41 (m, 4H, Ar–H), 7.35 (m, 4H, Ar–H), 7.14 (t, 1H, J=2.1 Hz, Ar–H), 2.36 (s, 3H, CH_3); ^{13}C NMR (75 MHz $CDCl_3$); δ (ppm): 185.1 (C=S), 168.4 (C=O), 140.5, 138.6, 137.8, 135.9, 132.0, 131.5, 130.7, 129.1, 128.7, 128.2, 127.9, 127.7, 127.4 (Aromatic-Cs), 21.5 (Ar-CH_3).

N-([1,1′-Biphenyl]-2-ylcarbamothioyl)-2-nitrobenzamide (3b)

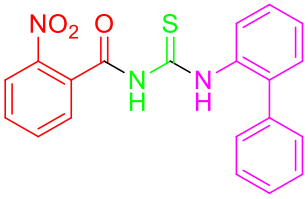

Light yellow solid, m.p.= 190-191 °C, Yield= 87 %, R_f= 0.47 (n-Hexane: Ethyl acetate 4:1); IR (KBr, v/cm^{-1}): 3325 (NH), 3165 (NH), 1668 (C=O), 1585, 1462 (C=C aromatic), 1234 (C=S), 1554, 1338 (N=O); ^{1}H NMR ($CDCl_3$, 300 MHz,); δ (ppm): 11.75(s, 1H, NH), 9.49 (s, 1H, NH), 8.45 (d, 1H, J=7.5 Hz, Ar–H), 8.29 (m, 2H, Ar–H), 7.57 (dd,1H, J=7.8 Hz, Ar–H), 7.33-7.40 (m, 4H, Ar–H), 7.37 (m, 4H, Ar–H), 7.15 (t, 1H, J=2.1 Hz, Ar–H); ^{13}C NMR (75 MHz $CDCl_3$); δ (ppm): 180.1 (C=S), 166.4 (C=O), 138.3, 138.1, 136.8, 135.5, 133.0, 131.8, 130.4, 130.2, 129.5, 128.9, 128.4, 128.0, 127.7, 127.6, 127.5, 127.4 (Aromatic-Cs).

N-([1,1′-Biphenyl]-2-ylcarbamothioyl)-3,5-dinitrobenzamide (3c)

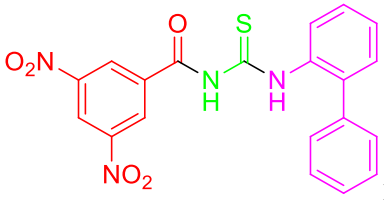

Light brown solid, m.p.= 200-201 °C, Yield= 81 %, R_f= 0.42 (n-Hexane: Ethyl acetate 4:1); IR (KBr, v/cm^{-1}): 3321 (NH), 3155 (NH), 1659 (C=O), 1575, 1460 (C=C aromatic), 1224 (C=S), 1559, 1340 (N=O); ^{1}H NMR ($CDCl_3$, 300 MHz,); δ (ppm): 12.11(s, 1H, NH), 9.65 (s, 1H, NH), 8.91 (d, 2H, J= 2.1 Hz, Ar–H), 8.86 (s, 1H, Ar–H), 7.30-7.40 (m, 4H, Ar–H), 7.35 (m, 4H, Ar–H), 7.14 (t, 1H, J= 2.1 Hz, Ar–H); ^{13}C NMR (75 MHz $CDCl_3$); δ (ppm): 180.1 (C=S), 166.4 (C=O), 138.3, 138.1, 136.8, 135.5, 133.0, 131.8, 130.4, 130.2, 129.5, 128.9, 128.4, 128.0, 127.7, 127.6, 127.5, 127.4 (Aromatic-Cs).

N-([1,1′-Biphenyl]-2-ylcarbamothioyl)-2-bromobenzamide (3d)

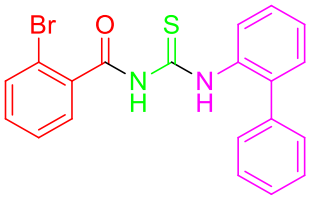

Greyish black solid, m.p.= 188-189 °C, Yield= 82 %, R_f = 0.40 (n-Hexane: Ethyl acetate 4:1); IR (KBr, v/cm^{-1}): 3315 (NH), 3105 (NH), 1651 (C=O), 1577, 1465 (C=C aromatic), 1230 (C=S); ^{1}H NMR ($CDCl_3$, 300 MHz,); δ (ppm): 11.95 (s, 1H, NH), 9.43 (s, 1H, NH), 7.91 (d, 2H, J= 7.9 Hz, Ar–H), 7.76 (d, 2H, J= 7.5 Hz, Ar–H), 7.57-7.59 (m, 2H, Ar–H), 7.27-7.39 (m, 4H, Ar–H), 7.33 (m, 4H, Ar–H), 7.12 (t, 1H, J= 2.1 Hz, Ar–H); ^{13}C NMR (75 MHz $CDCl_3$); δ (ppm): 185.1 (C=S), 168.4 (C=O), 138.3, 138.1, 136.8, 135.5, 133.0, 131.8, 130.4, 130.2, 129.5, 128.7, 128.2, 128.0, 127.6, 127.4, 127.1, 126.8 (Aromatic-Cs).

N-([1,1′-Biphenyl]-2-ylcarbamothioyl)butyramide (3e)

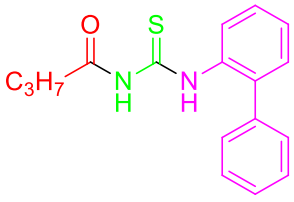

Grey solid, m.p.= 95-97 °C, Yield= 85 %, R_f= 0.51 (n-Hexane: Ethyl acetate 4:1); IR (KBr, v/cm^{-1}): 3325 (NH), 3179 (NH), 1681 (C=O), 1583, 1460 (C=C aromatic), 1229 (C=S); ^{1}H NMR ($CDCl_3$, 300 MHz,); δ (ppm): 12.12 (s, 1H, NH), 10.37 (s, 1H, NH), 7.35-7.42 (m, 4H, Ar–H), 7.39 (m, 4H, Ar–H), 7.79 (d, 1H, J= 7.1 Hz, Ar–H), 2.36 (t, 2H, J= 2.3), 2.26 (q, 2H), 0.97 (t, 3H); ^{13}C NMR (75 MHz $CDCl_3$) δ (ppm) 180.9 (C=S), 174.5 (C=O), 138.7, 138.2, 135.8, 135.5, 130.2, 128.5, 128.3, 128.2, 127.6, 127.5, 127.4 (Aromatic-Cs), 37.2, 24.4, 13.2 (n-butyl, C).

N-([1,1′-Biphenyl]-2-ylcarbamothioyl)pentanamide (3f)

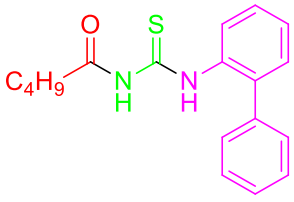

Colorless crystals, m.p.= 103-104 °C, Yield= 80 %, R_f= 0.53 (n-Hexane: Ethyl acetate 4:1); IR (KBr, v/cm^{-1}): 3321 (NH), 3187 (NH), 1685 (C=O), 1581, 1454 (C=C aromatic), 1224 (C=S); ^{1}H NMR ($CDCl_3$, 300 MHz,); δ (ppm): 12.14 (s, 1H, NH), 10.38 (s, 1H, NH), 7.36-7.45 (m, 4H, Ar–H), 7.40 (m, 4H, Ar–H), 7.81 (d, 1H, J= 7.1 Hz, Ar–H), 2.46 (t, 2H, J= 2.3), 1.57 (q, 2H), 1.33 (q, 2H), 0.90 (t, 3H); ^{13}C NMR (75 MHz $CDCl_3$) δ (ppm) 180.8 (C=S), 174.8 (C=O), 138.5, 138.0, 135.6, 130.1, 128.9, 128.3, 128.2, 127.6, 127.5, 127.5, 127.3 (Aromatic-Cs), 35.8, 26.7, 21.8, 13.1 (n-pentyl, C).

N-([1,1′-Biphenyl]-2-ylcarbamothioyl)heptanamide (3g)

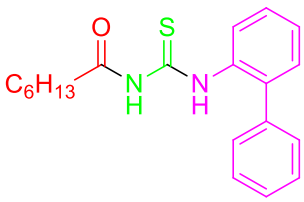

Colorless crystals, m.p.= 115-117 °C, Yield= 82 %, R_f= 0.54 (n-Hexane: Ethyl acetate 4:1); IR (KBr, v/cm^{-1}): 3325 (NH), 3185 (NH), 1659 (C=O), 1572, 1463 (C=C aromatic), 1230 (C=S); ^{1}H NMR ($CDCl_3$, 300 MHz,); δ (ppm): 12.16 (s, 1H, NH), 10.39 (s, 1H, NH), 7.29-7.44 (m, 4H, Ar–H), 7.35 (m, 4H, Ar–H), 7.61 (d, 1H, J= 7.1 Hz, Ar–H), 2.33 (t, 2H, J= 2.3), 1.57 (q, 2H), 1.29 (m, 6H), 0.91 (t, 3H); ^{13}C NMR (75 MHz $CDCl_3$) δ (ppm) 180.8 (C=S), 174.8 (C=O), 138.5, 138.0, 135.6, 130.1, 128.9, 128.3, 128.2, 127.6, 127.5, 127.5, 127.3 (Aromatic-Cs), 35.8, 26.7, 21.8, 13.1 (n-heptyl, C).

N-([1,1′-Biphenyl]-2-ylcarbamothioyl)octanamide (3h)

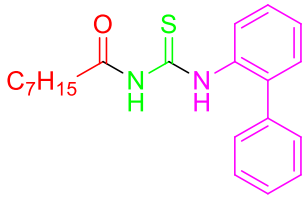

Colorless crystals, m.p.= 123-125 °C, Yield= 82 %, R_f= 0.54 (n-Hexane: Ethyl acetate 4:1); IR (KBr) v/cm^{-1}): 3331 (NH), 3181 (NH), 1659 (C=O), 1580, 1470 (C=C aromatic), 1227 (C=S); ^{1}H NMR ($CDCl_3$, 300 MHz,); δ (ppm): 12.19 (s, 1H, NH), 10.45 (s, 1H, NH), 7.29-7.41 (m, 4H, Ar–H), 7.33 (m, 4H, Ar–H), 7.60 (d, 1H, J= 7.1 Hz, Ar–H), 2.35 (t, 2H, J= 2.3), 1.18 (q, 2H), 1.62 (q, 2H), 1.31 (m, 6H) 0.89 (t, 3H, CH_3); ^{13}C NMR (75 MHz $CDCl_3$) δ (ppm) 180.8 (C=S), 174.8 (C=O), 138.5, 138.0, 135.6, 130.1, 128.9, 128.3, 128.2, 127.6, 127.5, 127.5, 127.3 (Aromatic-Cs), 35.8, 26.7, 21.8, 13.1 (n-octyl, C).

2.2- In vitro Methodology

2.2.1-Elastase inhibition assay

The elastase (from porcine pancreas) activity was determined following previously revealed technique by [28-29] with few adjustments. To play out the restraint of elastase movement, the measure of delivered p-nitroaniline, which was hydrolyzed from the substrate (N-succinyl-Ala-Ala-Ala-p-nitroanilide) by elastase, was dictated by estimating the absorbance at 410 nm. In detail, 0.8 mM arrangement of N-succinyl-Ala-Ala-Ala-p-nitroanilide was set up in a 0.2 M Tris-HCl cushion (pH 8.0) and this support (130 µL) was added to the test (10 µL) in a 96 well microplate. The microplate was pre-hatched for 10 min at 25 ºC before an elastase (0.0375 Unit/mL) stock arrangement (10 µL) was added. After catalyst expansion, the microplate was kept at 25 ºC for 30 min, and the absorbance was estimated at 410 nm utilizing microplate reader (SpectraMax ABS, USA). IC_{50} esteems were determined by nonlinear relapse utilizing GraphPad Prism 5.0 (GraphPad, San Diego, CA USA). All tests were done in three-fold. The elastase hindrance exercises were determined by the accompanying recipe:

$$Elastase\ inhibition\ \ activity\ (\%) = \left(OD_{control} - OD_{sample} \times 100\right)/OD_{control}$$

Where $OD_{control}$ and OD_{sample} signifies the optical densities in the lack and existence of sample, respectively. Oleanolic acid was used as the standard inhibitor for elastase.

2.2.2-Protocol for Kinetics

Kinetic analysis was carried out to determine the mode of inhibition by following our optimized method [30]. The compound **3c** was selected on the basis of its high IC_{50} value. Kinetics were carried out by varying the concentration of N-succinyl-Ala-Ala-Ala-p-nitroanilide from 2, 1, 0.5, 0.25, 0.125 and 0.0625 mM in the presence of different concentrations of compound **3c** (0.00, 0.25 and 0.51 µM) following the same procedure for the kinetic study as described in elastase inhibition assay protocol. Maximal initial velocities were determined from initial linear portion of absorbances

up to 10 minutes after addition of enzyme at per minute interval. The inhibition type on the enzyme was assayed by Lineweaver-Burk plot of inverse of velocities (1/V) versus inverse of substrate concentration 1/[S] mM^{-1}. The EI dissociation constant K_i was determined by secondary plot of 1/V versus inhibitor concentration. The results were processed by using SoftMaxPro.

2.3-X-ray diffraction data

The measurements were performed on an Oxford Xcalibur, Eos, Gemini CCD diffractometer with graphite-monochromated MoKα (λ= 0.71073 Å) radiation. X-ray diffraction intensities were collected (ω scans with ϑ and κ-offsets), integrated and scaled with CrysAlisPro [31] suite of programs. The unit-cell parameters were obtained by least-squares refinement (based on the angular settings for all collected reflections with intensities larger than seven times the standard deviation of measurement errors) using CrysAlisPro. Data were corrected empirically for absorption employing the multi-scan method implemented in CrysAlisPro. The structures were solved by intrinsic phasing with SHELXT [32] and the non-H molecular model refined with SHELXL [33]. All hydrogen atoms of **3f** but the methyl ones were located in a difference Fourier map and refined at their found positions with isotropic displacement parameters. The methyl H-atoms were positioned geometrically and refined with the riding model, treating the $-CH_3$ moieties as rigid groups allowed to rotate around the C–CH_3 bonds such as to maximize the sum of the residual electron density at the hydrogen calculated positions. Because libration disorder of the pendant alkane arm, C-C bond distances of **3h** were restrained to be equal during the refinement. All H-atoms were located at their expected positions and refined with the riding model. Crystal data and structure refinement results are summarized in **Tables S1-S7** (Supporting Information)**.** Crystallographic structural data have been deposited at the Cambridge Crystallographic Data Centre (CCDC) with reference numbers CCDC 2058591 (**3f**) and CCDC 2058592 (**3h**).

2.4- Computational Methodology

2.4.1-Retrieval of porcine pancreatic elastase structure.

The crystal structure of porcine pancreatic elastase was accessed from Protein Data Bank (PDB) (www.rcsb.org) with PDBID 7EST and the protein structure was minimized by using UCSF Chimera 1.6rc [34-35]**.** The stereo-chemical properties of elastase and Ramachandran plot and values were also accessed from PDB. The hydrophobicity graph of target protein was generated by Discovery Studio 4.1 Client [36].

2.4.2- Designing of synthesized compounds and molecular docking

The structures of compounds **(3a-h)** were sketched in ACD/ChemSketch and the UCSF Chimera 1.10.1 tool was employed to energy minimization of each ligand separately having default parameters such as steepest descent steps 100 with step size 0.02 (Å), conjugate gradient steps 100 with step size 0.02 (Å) and update interval was fixed at 10. Finally, Gasteiger charges were added using Dock Prep in ligand structure to obtain the good structure conformation. Molecular docking experiment of compounds **(3a-h)** against the porcine pancreatic elastase were done by using virtual screening tool PyRx with VINA Wizard approach [37]. The grid box parameters values in VINA search space (X= 4.6898, Y= 57.6015 and Z= -5.7255) were adjusted with default exhaustiveness value = 8 to maximize the binding conformational analysis. We have adjusted sufficient grid box size on biding pocket residues to allow the ligand to move freely in the search space. All the synthesized ligands were docked separately against target protein. In all docked complexes, the ligands conformational poses were keenly observed to obtain the best docking results. The generated docked complexes were evaluated based on lowest binding energy (kcal/mol) values and binding interaction pattern between ligands and receptor. The graphical depictions of all the docked complexes were accomplished by UCSF Chimera 1.10.1 and Discovery Studio (2.1.0), respectively.

3- Results and Discussion

3.1. Synthesis and Characterization

In **Scheme 1** the synthetic pathway for aliphatic and aromatic derivatives *N*-([1,1′-biphenyl]-2-ylcarbamothioyl)-substituted benzamide and *N*-([1,1′-biphenyl]-2-ylcarbamothioyl)-alkylamide derivatives is described. Reaction of freshly prepared acyl/aryl 1-carbonyl isothiocyanates with 2-aminobiphenyl furnished the target compounds in good yields (higher than 80 %) and high purity.

The synthetized thiourea derivatives are characterized by their physical parameters, FTIR and NMR spectroscopic techniques. In the infrared spectra, the characteristic peaks for N-H stretching appear as broad absorptions in the range of 3355-3185 cm^{-1}. This feature is in agreement with previous reports on vibrational properties of 1-acyl-3-monosubtituted thioureas, with the N-H stretching modes of the thioamide group being shifted to lower frequencies due to the formation of intramolecular N-H•••O=C hydrogen bond [25]. This interaction also affects the C=O stretching mode, which is observed as intense and well-defined band in the range 1685-1650 cm^{-1} [26]. The biphenyl group is characterized by the presence of aromatic C=C stretching frequencies are observed at 1585-1473 cm^{-1} and the C=S group absorbs at 1253-1227 cm^{-1}.

In ^{1}H NMR spectra, the two characteristic N-H protons signals appeared in the range of δ= 12.16-11.75 and δ= 10.45-9.41 ppm. The N-H proton connected to the electrophilic functional groups (carbonyl and thiocarbonyl) is more deshielded as compare to the N-H proton is connected to the thiocarbonyl moiety [27]. The low-field resonance observed for the thioamide proton is a signature for the occurrence of intramolecular N-H•••O=C hydrogen interaction, as discussed below. The aromatic region protons were observed from δ= 7.86-7.35 ppm and the aliphatic region protons signals appeared in the range of δ= 2.29-0.91 ppm, as expected.

In ^{13}C NMR, two differentiating signals of thiocarbonyl and carbonyl carbons appeared at δ= 185.1-179.6 and δ= 174.8-165.4 ppm, respectively. The difference in shift values between C=O and C=S groups is due to the presence of the NH groups that exert electron withdrawing effect. The aromatic carbon nucleus of the byphenyl group resonates in the range ca. 138-126 ppm and the alkyl chains are observed at higher fields, as expected.

3.2- Structural results

ORTEP [38] plots of the solid state **3f** and **3h** molecules are shown in Figure 1 and corresponding selected bond distances and angles are reported in **Table 1**. The **3f**-containing solid incorporated an acetone solvent molecule sited on a crystallographic two-fold axis and therefore it should be formulated as **3f**.½$CH_3(CO)CH_3$. As expected, both compounds show closely related molecular structures, only differing in the length of the alkyl pendant arm. In fact, the rms deviation between homologous non-H atoms in the best least-squares structural fitting of the common skeletal framework (calculated by the Kabsh procedure [39]) is less than 0.15 Å. An intramolecular N1H•••O bond [d(N•••O) = 2.613(3) Å and ∠(N-H•••O)=140(2)º for **3f** and d(N•••O) = 2.663(3) Å and ∠(N-H•••O) = 136º for **3h**] promotes a nearly planar 1-acyl thiourea group, as usual for mono-substituted 1-acyl thioureas [40,41]. Within this group of the better refined **3f** compound, observed d(C_{ph}-N) = 1.418(3) Å, SC-N bond distances of 1.325(3) and

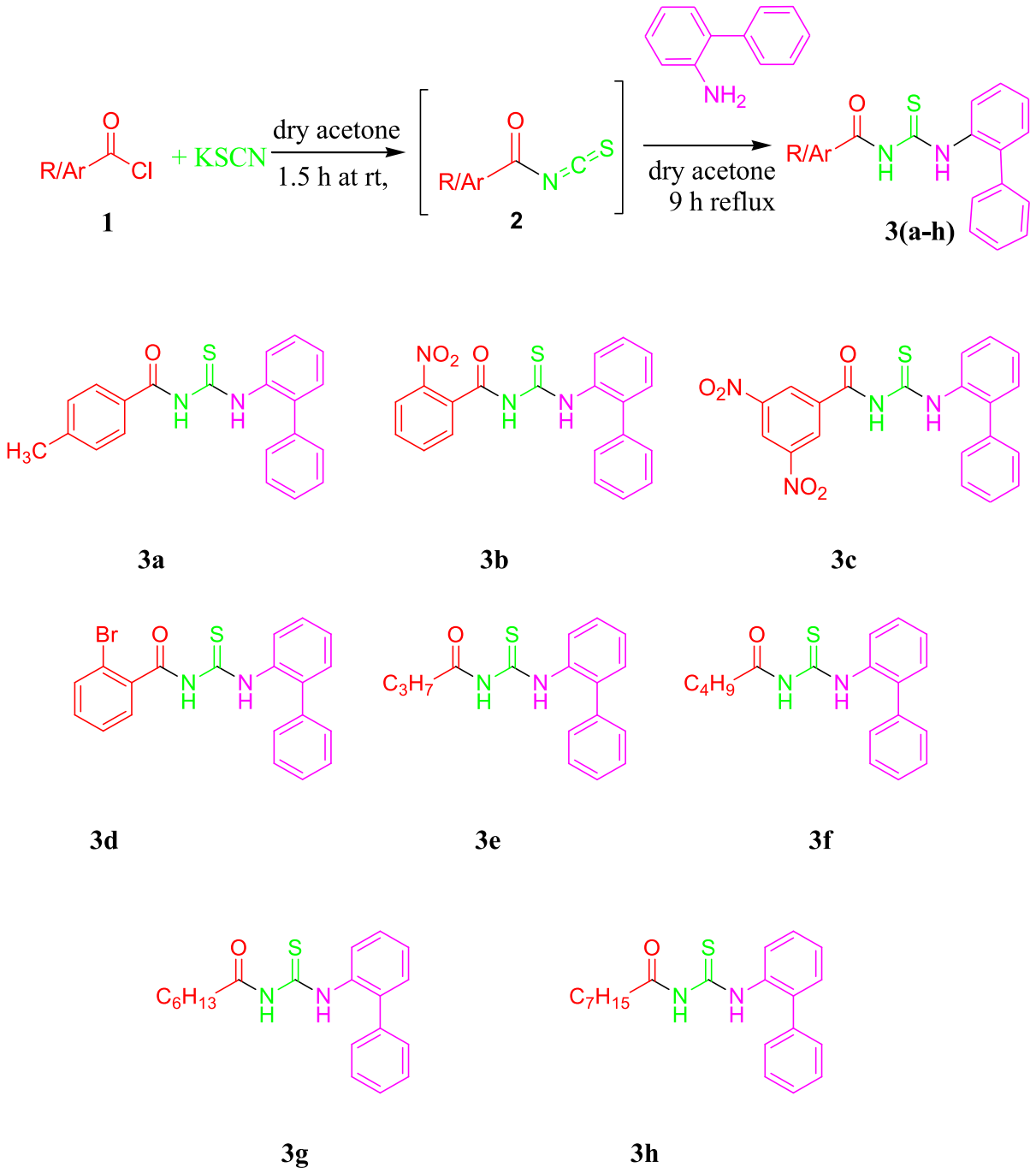

Scheme 1. Synthetic route and structures of the thiourea derivatives (**3a-h**).

Table 1
Selected bond lengths [Å] and angles [°] in *N*-([1,1′-Biphenyl]-2-ylcarbamothioyl)pentanamide (**3f**) in **3f**.½$CH_3(CO)CH_3$ and *N*-([1,1′-Biphenyl]-2-ylcarbamothioyl)octanamide (**3h**).[a]

0Parameter	3f	3h	Parameter	3f	3h
C14=O1	1.223(3)	1.229(3)	O1=C14-N2	122.0(2)	122.2(2)
C14-N2	1.378(3)	1.359(3)	O1=C14-C15	121.9(2)	122.2(2)
C13-N2	1.381(3)	1.402(3)	C14-N2-C13	128.1(2)	129.4(2)
C13=S1	1.672(2)	1.659(2)	N2-C13=S1	118.0(2)	118.1(2)
C13-N1	1.325(3)	1.324(3)	N2-C13-N1	115.9(2)	115.5(2)
N1-C1	1.418(3)	1.428(3)	S1=C13-N1	124.5(2)	126.4(2)
C14-C15	1.490(4)	1.498(4)	C13-N1-C1	126.6(2)	125.3(2)

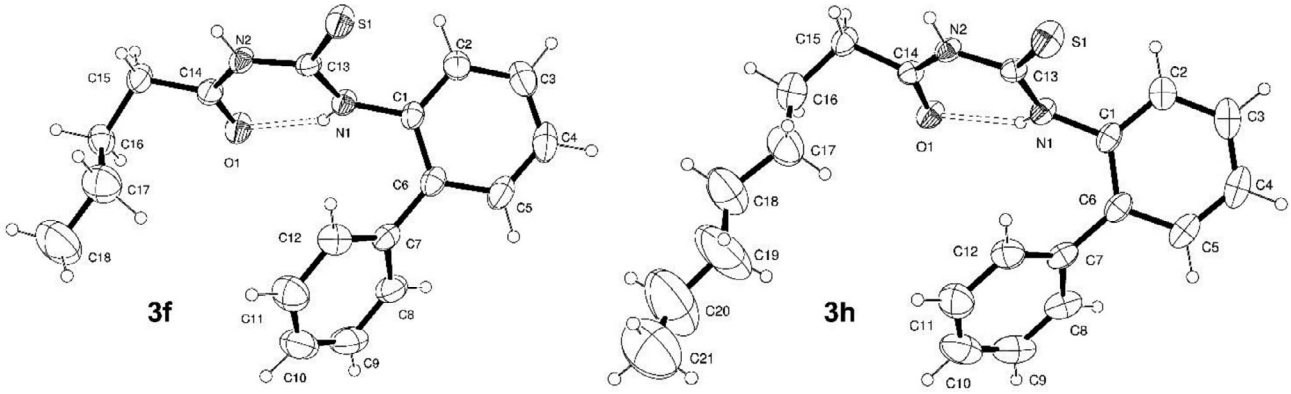

Fig. 1. Drawings of solid state **3f** and **3h** molecules showing the labeling of the non-H atoms and their displacement ellipsoids at the 30% probability level. The intramolecular H-bonds are indicated by dashed lines.

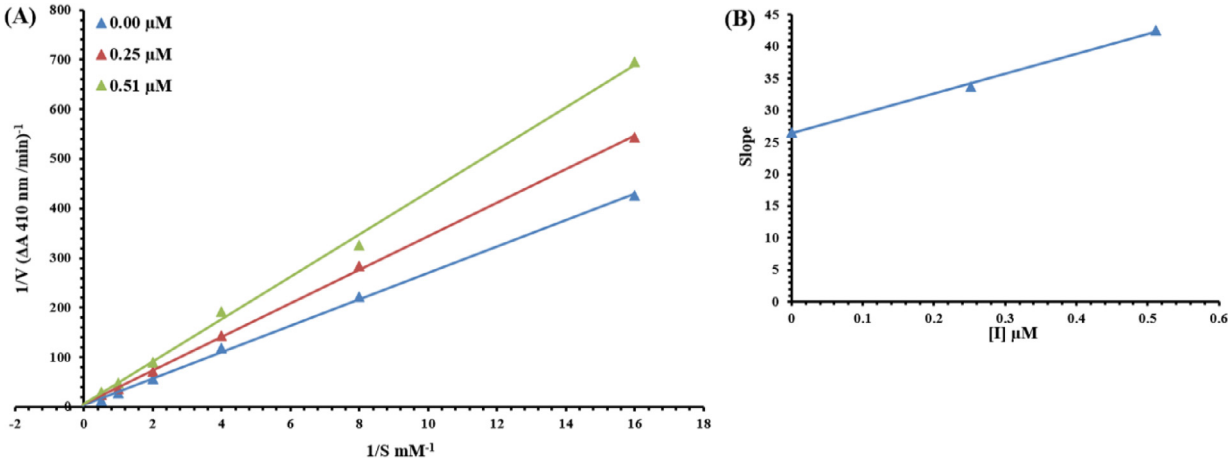

Fig. 2. Lineweaver–Burk plots for inhibition of elastase in the presence of compound **3c** (A). Concentrations of **3c** used were 0.00, 0.25 and 0.51 µM. Substrate *N*-succinyl-Ala-Ala-Ala-p-nitroanilide concentrations were 2, 1, 0.5, 0.25, 0.125 and 0.0625 mM. (B) The insets represent the plot of the slope.

1.381(3) Å, and d(OC-N) = 1.378(3) Å confirm the single-bond character of C-N links. Double C=S and C=O bond lengths are 1.672(2) and 1.223(3) Å, respectively.

The crystals are further stabilized by intermolecular H-bonds. In fact, **3h** is arranged as centrosymmetric dimers, linked through N2–H•••S bonds [d(N•••S') = 3.447(2) Å and ∠(N–H•••S') = 171(2)º] given rise to a R crystal motif [42]. Neighboring molecules in the **3f** lattice are linked to each other through N2–H•••O bonds [d(N•••O') = 2.874(3) Å and ∠(N–H•••O') = 156.5º], giving rise to a polymeric chain that extends along the crystal c-axis. These H-bonding structures are further detailed in the supplementary Information (Tables S6 a and b, for **3f** and **3h**, respectively).

[a] For atom numbering see Figure 1.

3.3- In-vitro Inhibitory Activity

All of the synthesized compounds were tested in vitro for their elastase inhibitory activity. Five different concentrations were used for calculation of IC_{50} (Table 2), including the standard oleanolic acid. It is evident from the IC_{50} values that in general compounds bearing aryl groups (**3a-3d**) have superior activity than those having alkyl substitution (**3e-3h**). Thus, the IC_{50} values of 0.284 ± 0.077 and 0.255 ± 0.049 μM are determined for most active **3b** and **3c** compounds, respectively, whereas the IC_{50} for the alkylated thioureas **3a-3d** are in the range 0.9-1.3 μM. The analysis of the substituent effect shows that presence of electron withdrawing substituents such as nitro (**3b** and **3c**) and bromo (**3d**) are more effective inhibitors those with electron donating methyl group (**3a**). In particular, the influence of nitro groups in the activity of compounds 3b and 3c will be further determined by using docking analysis.

Table 2
IC_{50} values (in μM) for the elastase (elastase from porcine pancreas) inhibitory activity of derivatives (**3a-3h**).

Compound	IC_{50}±SEM (μM)	Compound	IC_{50}±SEM (μM)
3a	0.915 ± 0.614	**3e**	1.328 ± 0.993
3b	0.284 ± 0.077	**3f**	0.979 ± 0.655
3c	0.255 ± 0.049	**3g**	0.997 ± 0.847
3d	0.518 ± 0.471	**3h**	0.942 ± 0.881
Oleanolic Acid	13.451 ± 0.014		

SEM = Standard error of the mean; values are expressed in mean ± SEM.

3.4-Kinetic Studies

The kinetic study was performed to understand the inhibitory mode of compound **3c** against elastase. Based upon results of IC_{50} data the most potent compound **3c** was selected for determination of inhibition type and inhibition constant. The kinetic results of the enzyme by the Lineweaver-Burk plot of 1/V versus substrate N-succinyl-Ala-Ala-Ala-p-nitroanilide 1/[S] in the presence of different inhibitor concentrations gave a series of straight lines, the result for compound **3c** showed that V_{max} remains the same without significantly effecting the slopes. K_m increases with increasing concentration while V_{max} remains the same only with minor dif-

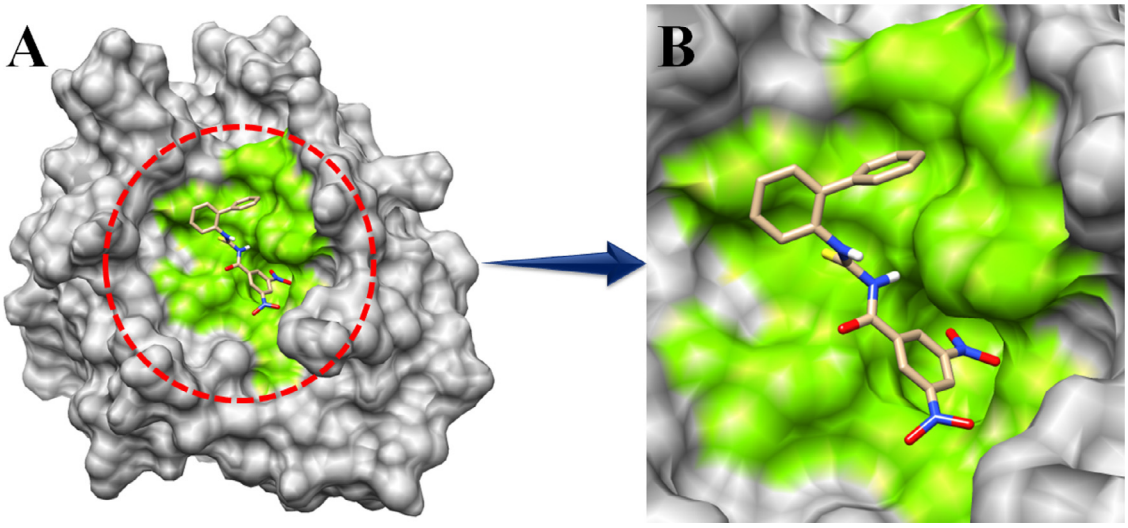

Fig. 3. A, B. Binding pocket of elastase with embedded ligand **3c.**

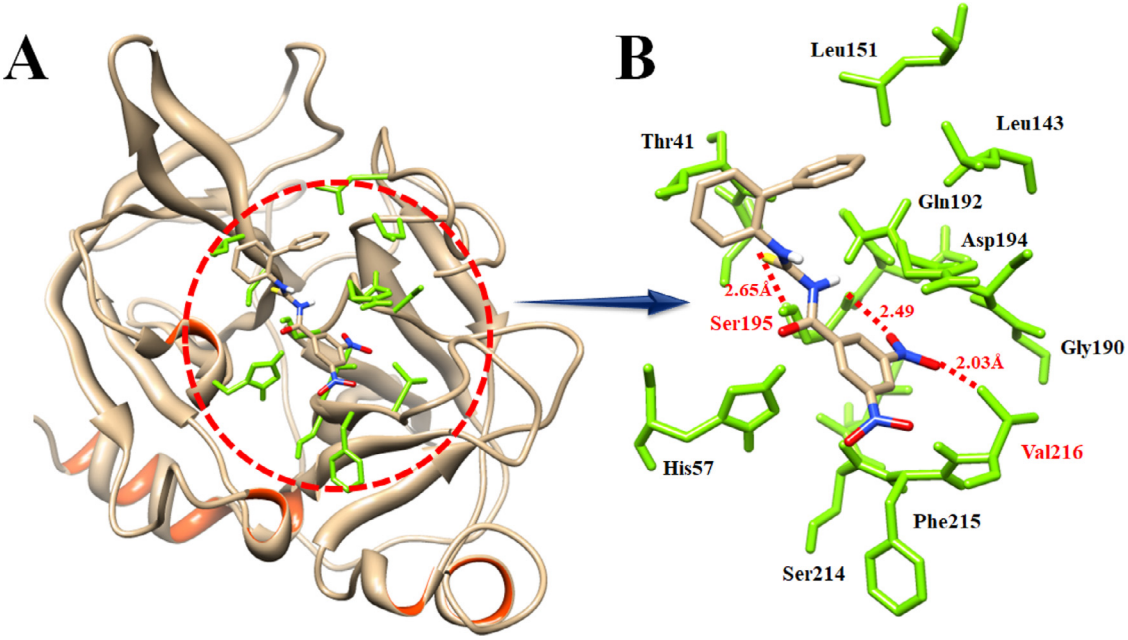

Fig. 4. Molecular docking interaction of **3c** against receptor molecule. **A**) The general overview of docking depiction. **B**) The closer view of binding pocket interaction with best conformation position of ligand against target protein. The interacted amino acids are highlighted in green color and red dotted lines with distance mentioned in angstrom (Å) are justified for H-bond distances.

ference. This behavior indicates that **3c** compound inhibits the enzymes in a competitive manner (Figure 2. A), second plot (Figure 2. B) of slope against concentration of **3c** showed EI dissociation constant. The K_i calculated from inhibitor concentration of **3c** versus the slope was found to be 0.84 µM.

3.5- Molecular docking analysis

Porcine pancreatic elastase consists of 240 amino acids having calcium atom inserted in the protein structure. The Ramachandran graph shows 88.70 % of residues were present in favored region whereas 98.70% residues remain in allowed region. The Ramachandran plot of porcine pancreatic elastase is revealed in supplementary data Fig S1.

To predict the top suited conformational position of synthesized compounds **(3a-h)** within the active region of elastase enzyme, docking studies were carried. The results indicated that all compounds possess energy values in the range -5.9 to -7.6 Kcal/mol (Table 3)**.** The docking energy values were calculated by employing equation 1:

Table 3
The docking energy values.

Docking Complexes	Binding Affinity (kcal/mol)
3a	-6.7
3b	-7.6
3c	-7.7
3d	-6.7
3e	-5.9
3f	-6.3
3g	-6.6
3h	-6.6

$$\Delta Gbinding = \Delta Ggauss + \Delta Grepulsion + \Delta Ghbond + \Delta Ghydrophobic + \Delta Gtors \quad \text{(eq. 1)}$$

Here, ΔGgauss: attractive term for dispersion of two gaussian functions, ΔGrepulsion: square of the distance if closer than a threshold value, ΔGhbond: ramp function - also used for interactions with metal ions, ΔGhydrophobic: ramp function, ΔGtors: proportional to the number of rotatable bonds.

In docking results compounds having more than 2.5 kcal/mol energy are thought as potent for inhibition of target enzyme. The standard error for Autodock is reported as 2.5 kcal/mol (http://autodock.scripps.edu/). Present docking results vindicated that the energy value difference among all docking complexes were smaller than standard error. Therefore, based on both in vitro and in silico docking energy results, compound **3c** was rated as the best ligand with good inhibitory potential compared to rest of the derivatives here studied and related compounds already reported [43]. Given that the basic scaffold of all the synthesized compounds was identical consequently, most of ligands possess good energy values without any major difference.

3.6- Binding pocket and ligand conformation

The binding pocket analysis revealed that compound **3c** binds in excellent conformational position and best fitted in the binding pocket of elastase. The amino group on the benzene ring in **3c** showed their binding pattern in the deep region of binding cavity, whereas rest of benzene rings were confined in the central part of binding pocket (Figure 3 A, B).

The docked complexes were analyzed based on H-bonding and hydrophobic contacts. The best in vitro result compound **(3c)** was selected to check best conformational position inside active region of target protein. As shown in Figure 4, the ligand retains nearly the same conformation in the protein pocket. The **3c** form three H-bonds with different residues of the protein: sulfur forms H-bonds with Ser195 with bond length of 2.65 Å and the oxygen atoms of nitro groups form two H-bonds with Ser195 and Val216 having bonds distance 2.49 and 2.03 Å, respectively in line with reported data [44]. The rest of docking complexes are given in supplementary data (Fig S2-S8).

4-Conclusions

An efficient synthesis of novel 1-acyl thiourea-biphenyl hybrids is described by treating aryl/alkyl-carbonyl isothiocyanate with 2-aminobiphenyl in good yields. Crystal X-ray diffraction analysis for two alkylated derivatives, namely **3f** and **3h**, shows that the central –C(O)NHC(S)NH– moiety adopts a typical six-membered ring structure, a conformation favored by a strong N–H•••O=C intramolecular hydrogen bond.

In vitro studies showed that the aryl-substituted derivatives exhibit significant elastase inhibitor activity. Compound **3c** proved to be the most active with IC_{50} value of 0.26±0.05 μM. Its mode of inhibition was competitive, with dissociation constant K_i = 0.84 µM. Molecular docking at the enzyme active site was carried out to study enzyme-inhibitor interactions. The existence of H-bonds between **3c** with different residues in the protein pocket indicated the sulfur atom of thiourea forming a C=S•••H hydrogen bond with Ser195 and the oxygen of the acyl group form two C=O•••H, H-bonds with Ser195 and Val216. These interactions appear to be likely for a strong binding energy (-7.70 kcal/mol) between **3c** and the elastase.

Declaration of Competing Interest

The authors declare that they have no known competing financial interests or personal relationships that could have appeared to influence the work reported in this paper.

CRediT authorship contribution statement

Sara Ilyas: Data curation, Formal analysis, Investigation, Methodology, Software, Validation, Visualization. **Aamer Saeed:** Conceptualization, Data curation, Formal analysis, Funding acquisition, Investigation, Methodology, Project administration, Resources, Software, Supervision, Validation. **Qamar Abbas:** Data curation, Formal analysis, Investigation, Methodology, Software, Validation, Visualization. **Rabail Ujan:** Data curation, Formal analysis, Investigation, Methodology, Software, Validation, Visualization. **Pervaiz Ali Channar:** Data curation, Formal analysis, Investigation, Methodology, Software, Validation, Visualization. **Izhar Ahmed Shaikh:** Data curation, Formal analysis, Investigation, Methodology, Software, Validation, Visualization. **Mubashir Hassan:** Data curation, Formal analysis, Investigation, Methodology, Software, Validation, Visualization. **Hussain Raza:** Data curation, Formal analysis, Investigation, Methodology, Software, Validation, Visualization. **Sung-Yum Seo:** Data curation, Formal analysis, Investigation, Methodology, Software, Validation, Visualization. **Gustavo A. Echeverría:** Data curation, Formal analysis, Investigation, Methodology, Resources, Software, Validation, Visualization. **Oscar E. Piro:** Data curation, Formal analysis, Investigation, Methodology, Resources, Software, Validation, Visualization. **Mauricio F. Erben:** Conceptualization, Data curation, Formal analysis, Funding acquisition, Investigation, Methodology, Project administration, Resources, Software, Supervision, Validation.

Acknowledgments

Argentinean authors thank the CONICET (Grant PIP 0651), the ANPCyT (PICT-2019-2578) and UNLP (Grants 11/X709, 11/X857, and 11/X794) for financial support. GAE, MFE, and OEP are Research Fellows of CONICET.

Supplementary materials

Supplementary material associated with this article can be found, in the online version, at doi:10.1016/j.molstruc.2021.130993.

References

[1] A. Saeed, R. Qamar, T.A. Fattah, U. Flörke, M.F. Erben, Res. Chem. Intermed. 43 (5) (2017) 3053–3093.
[2] M. Atis,, F. Karipcin, B. Sarıboga, M. Tas, H. Celik, Spectrochim. Acta Mol. Biomol. Spectrosc. 98 (2012) 290–301.
[3] A. Saeed, M.N. Mustafa, M. Zain-ul-Abideen, G. Shabir, M.F. Erben, U. Flörke, J. Sulfur Chem. 40 (3) (2019) 312–350.
[4] S. Murru, C.B. Singh, V. Kavala, B.K. Patel, Tetrahedron 64 (2008) 1931–1942.
[5] X.-P. Rao, Y. Wu, Z.-Q. Song, S.-B. Shang, Z.-D. Wang, Med. Chem. Res. 20 (2011) 333–338.
[6] S.-Y. Ke, S.-J. Xue, Arkivoc 10 (2006) 63–68.
[7] J.R. Burgeson, A.L. Moore, J.K. Boutilier, N.R. Cerruti, D.N. Gharaibeh, C.E. Lovejoy, S.M. Amberg, D.E. Hruby, S.R. Tyavanagimatt, R.D. Allen, Bioorg. Med. Chem. Lett. 22 (2012) 4263–4272.
[8] C. Limban, A.-V. Missir, I.C. Chirita, M.T. Caproiu, Rev. Chim. Bucharest. 61 (2010) 946–950.
[9] Z. Zhong, R. Xing, S. Liu, L. Wang, S. Cai, P. Li, Carbohydr. Res. 343 (2008) 566–570.
[10] J.-F. Zhang, J.-Y. Xu, B.-L. Wang, Y.-X. Li, L.-X. Xiong, Y.-Q. Li, Y. Ma, Z.-M. Li, J. Agric. Food Chem. 60 (2012) 7565–7572.
[11] S.Y. Abbas, M.A.S. El-Sharief, W.M. Basyouni, I.M. Fakhr, E.W. El-Gammal, Eur. J. Med. Chem. 64 (2013) 111–120.
[12] S. Saeed, N. Rashid, P.G. Jones, M. Ali, R. Hussain, Eur. J. Med. Chem. 45 (2010) 1323–1331.
[13] L.P. Duan, J. Xue, L.L. Xu, H.B. Zhang, Molecules 15 (2010) 6941–6947.

[14] M. Struga, S. Rosolowski, J. Kossakowski, J. Stefanska, Arch. Pharm. Res. 33 (2010) 47–54.
[15] D. Doğruer, Ş. Urlu, ; T. Önkol, B. Özçelik, M.F. Şahin, Turk. J. Chem. 34 (2010) 57–65.
[16] S. Ashraf, A. Saeed, M.A. Malik, U. Flörke, M. Bolte, N. Haider, J. Akhtar, Eur. J. Inorg. Chem. (2014) 533–538.
[17] S. Zaib, A. Saeed, K. Stolte, U. Flörke, M. Shahid, J. Iqbal, Eur. J Med. Chem. 78 (2014) 140–150.
[18] S. Cunha, C. F., Jr Macedo, G.A.N. Costa, M. T., Jr Rodrigues, R.B.V. Verde, L.C.de Souza Neta, I. Vencato, C. Lariucci, F.P. Sa, Monatsh. Chem. Chem. Mon. 138 (2007) 511–516.
[19] A. Saeed, U. Shaheen, A. Hameed, S.Z. Haider Naqvi, J. Fluor. Chem. 130 (2009) 1028–1034.
[20] A. Misra, M. Shahid, P. Dwivedi, Talanta 80 (2009) 532–538.
[21] A.M. Costero, G.M. Rodriguez-Muñiz, A.P. Gavi, S. Gil, A. Domenech, Tetrahedron Lett 48 (2007) 6992–6995.
[22] B.M. Yamin, M.A.M. Arif, Acta Cryst (2008) E64 o104–o104.
[23] M.A.M. Arif, B.M. Yamin, Acta Cryst (2007) E63 o3594–o3594.
[24] T. Yesilkaynak, G. Binzet, F.M. Emen, U. Flörke, N. Külcü, H. Arslan, Eur. J. Chem. 1 (2010) 2–6.
[25] A. Saeed, M.F. Erben, M. Bolte, J. Mol. Struct. 985 (2010) 57–62.
[26] A. Saeed, M.F. Erben, M. Bolte, Spectrochim. Acta A 102 (2013) 408–413.
[27] A. Saeed, A. Khurshid, J.P. Jasinski, C.G. Pozzi, A.C. Fantoni, M.F. Erben, Chem. Phys. 431 (2014) 39–46.
[28] S.S. Hamdani, B.A. Khan, A. Saeed, F.A. Larik, S. Hameed, P.A. Channar, K. Ahmad, E.U. Mughal, Q. Abbas, N.U. Amin, S.A. Ghumro, Archiv der Pharmazie 352 (8) (2019) 1900061.
[29] A. Saeed, D. Shahzad, F.A. Larik, P.A. Channar, H. Mahfooz, Q. Abbas, M. Hassan, H. Raza, S.Y. Seo, G. Shabir, Bangladesh J. Pharmacol. 12 (2) (2017) 25–2017.
[30] A.R.S. Butt, M.A. Abbasi, S.Z. Siddiqui, M. Hassan, H. Raza, S.A.A. Shah, S.Y. Seo, Bioorg. Chem. 86 (2019) 459–472.
[31] CrysAlisProRigaku Oxford Diffraction, Rigaku Corporation, Oxford, UK, 2015.
[32] G.M. Sheldrick, Acta Cryst A71 (2015) 3–8.
[33] G.M. Sheldrick, Acta Cryst A64 (2008) 112–122.
[34] E.F. Pettersen, T.D. Goddard, C.C. Huang, G.S. Couch, D.M. Greenblatt, J Comput Chem 25 (2004) 1605–1612.
[35] V.B. Chen, W.B. Arendall, J.J. Headd, D.A. Keedy, R.M. Immormino, Acta Crystallogr D Biol Crystallogr 66 (2010) 12–21.
[36] D Studio, Discovery. "version 2.1, Accelrys, San Diego, CA, 2008.
[37] S. Dallakyan, A.J. Olson, Mol Biol 1263 (2015) 243–250.
[38] L.J. Farrugia, J Appl Cryst 30 (1997) 565–566.
[39] W. Kabsch, Acta Cryst A32 (1976) 922923.
[40] D.L.N. González, A. Saeed, G. Shabir, U. Flörke, M.F. Erben, J. Mol. Struct. 1215 (2020) 128227.
[41] R.R. Cairo, A.M. Plutín Stevens, T.D. de Oliveira, A.A. Batista, E.E. Castellano, J. Duque, D.B. Soria, A.C. Fantoni, R.S. Corrêa, M.F. Erben, Spectrochim. Acta Part A: Mol. Biomol. Spectrosc. 176 (2017) 8–17.
[42] A. Saeed, M. Bolte, M.F. Erben, H. Pérez, CrystEngComm 17 (39) (2015) 7551–7563.
[43] M.Paola Giovannoni, I.A. Schepetkin, L. Crocetti, G. Ciciani, A. Cilibrizzi, G. Guerrini, A.I. Khlebnikov, M.T. Quinn, C. Vergelli, J. Enzyme Inhib. Med. Chem. 31 (4) (2016) 628–639.
[44] N.C. Dige, P.G. Mahajan, H. Raza, M. Hassan, B.D. Vanjare, H. Hong, K.H. Lee, S.Y. Seo, Bioorg. Chem. 100 (2020) 103906.